Fungal Biology 126 (2022) 35–46

Contents lists available at ScienceDirect

Fungal Biology

journal homepage: www.elsevier.com/locate/funbio

CRISPR-Cas9 gene editing and rapid detection of gene-edited mutants using high-resolution melting in the apple scab fungus, *Venturia inaequalis*

Mercedes Rocafort [a], Saadiah Arshed [b], Debbie Hudson [c], Jaspreet Singh Sidhu [c], Joanna K. Bowen [b], Kim M. Plummer [d], Rosie E. Bradshaw [e, f], Richard D. Johnson [c], Linda J. Johnson [c], Carl H. Mesarich [a, f, *]

[a] *Laboratory of Molecular Plant Pathology, School of Agriculture and Environment, Massey University, Palmerston North, 4410, New Zealand*
[b] *The New Zealand Institute for Plant and Food Research Limited, Mount Albert Research Centre, Auckland, 1025, New Zealand*
[c] *Grasslands Research Centre, AgResearch Limited, Palmerston North, 4410, New Zealand*
[d] *Department of Animal, Plant and Soil Sciences, La Trobe University, AgriBio, Centre for AgriBiosciences, La Trobe University, Bundoora, Victoria, 3086, Australia*
[e] *Laboratory of Molecular Plant Pathology, School of Fundamental Sciences, Massey University, Palmerston North, 4410, New Zealand*
[f] *The New Zealand Bio-Protection Research Centre, Massey University, Palmerston North, 4410, New Zealand*

ARTICLE INFO

Article history:
Received 24 February 2021
Received in revised form
27 September 2021
Accepted 7 October 2021
Available online 9 October 2021

Corresponding editor: Neil A Brown

Keywords:
CRISPR-Cas9 gene editing
Venturia inaequalis
Fungus
Apple scab
High-resolution melting
Trihydroxynaphthalene reductase gene
Melanin biosynthesis pathway

ABSTRACT

Apple scab, caused by the fungal pathogen *Venturia inaequalis*, is the most economically important disease of apple (*Malus* x *domestica*) worldwide. To develop durable control strategies against this disease, a better understanding of the genetic mechanisms underlying the growth, reproduction, virulence and pathogenicity of *V. inaequalis* is required. A major bottleneck for the genetic characterization of *V. inaequalis* is the inability to easily delete or disrupt genes of interest using homologous recombination. Indeed, no gene deletions or disruptions in *V. inaequalis* have yet been published. Using the melanin biosynthesis pathway gene *trihydroxynaphthalene reductase* (*THN*) as a target for inactivation, which has previously been shown to result in a light-brown colony phenotype when transcriptionally silenced using RNA interference, we show, for the first time, that the CRISPR-Cas9 gene editing system can be successfully applied to the apple scab fungus. More specifically, using a CRISPR-Cas9 single guide RNA (sgRNA) targeted to the *THN* gene, delivered by a single autonomously replicating Golden Gate-compatible plasmid, we were able to identify six of 36 stable transformants with a light-brown phenotype, indicating an ~16.7% gene inactivation efficiency. Notably, of the six *THN* mutants, five had an independent mutation. As part of our pipeline, we also report a high-resolution melting (HRM) curve protocol for the rapid detection of CRISPR-Cas9 gene-edited mutants of *V. inaequalis*. This protocol identified a single base pair deletion mutation in a sample containing only 5% mutant genomic DNA, indicating high sensitivity for mutant screening. In establishing CRISPR-Cas9 as a tool for gene editing in *V. inaequalis*, we have provided a strong starting point for studies aiming to decipher gene function in this fungus. The associated HRM curve protocol will enable CRISPR-Cas9 transformants to be screened for gene inactivation in a high-throughput and low-cost manner, which will be particularly powerful in cases where the CRISPR-Cas9-mediated gene inactivation efficiency is low.

1. Introduction

Fungal species from the *Venturia* genus are devastating plant pathogens of economically important crops that mainly belong to the *Rosaceae* (Bowen et al., 2011; González-Domínguez et al., 2017; Le Cam et al., 2019). The best researched of these pathogens is *Venturia inaequalis*, which causes scab, or black spot, the most

* Corresponding author. School of Agriculture and Environment, Massey University, Private Bag 11222, Palmerston North, 4442, New Zealand.
E-mail address: c.mesarich@massey.ac.nz (C.H. Mesarich).

https://doi.org/10.1016/j.funbio.2021.10.001

economically important disease of apple (*Malus* x *domestica*) worldwide (Bowen et al., 2011). Under favourable conditions, this disease can result in 70% or more of the crop being lost, as scab renders the apples unmarketable (i.e. through blemishes and deformation), and reduces both the growth and yield of the plant (i.e. by causing repeated defoliation of trees over several seasons) (Bowen et al., 2011; González-Domínguez et al., 2017; Jha et al., 2009). To develop durable control strategies against scab disease, a better understanding of the genetic mechanisms underlying the growth, reproduction, virulence and pathogenicity of *V. inaequalis* is required.

A key development over recent years has been the availability of several *V. inaequalis* genome sequences and gene catalogues (Deng et al., 2017; Le Cam et al., 2019; Lichtner et al., 2020; Papp et al., 2020; Passey et al., 2018, 2020), as well as the development of both polyethylene glycol (PEG)-mediated protoplast and *Agrobacterium tumefaciens*-mediated transformation protocols for use with this fungus (Fitzgerald et al., 2003). However, while several *V. inaequalis* genes of interest that are putatively involved in the infection process of apple have been identified (Bowen et al., 2009; Deng et al., 2017; Feurtey et al., 2020; Kucheryava et al., 2008; Mesarich et al., 2012; Shiller et al., 2015), none have been functionally characterized to date using traditional gene deletion or disruption techniques. Indeed, no gene deletions or disruptions have yet been reported for *V. inaequalis* in the literature. This suggests that gene deletion or disruption by traditional homologous recombination is extremely inefficient in *V. inaequalis*. It should be noted that transcriptional silencing of multiple genes in *V. inaequalis* has been achieved using RNA interference (RNAi) (Fitzgerald et al., 2004). However, RNAi does not typically silence a gene to completion and the observed phenotypes can be inconsistent, unclear or absent, making it difficult to determine function (Nakayashiki and Nguyen, 2008; Salame et al., 2011). Taken together, alternative gene disruption and deletion tools, such as the Clustered Regularly Interspaced Short Palindromic Repeats-Cas9 (CRISPR-Cas9) system (Doudna and Charpentier, 2014), are desperately needed to assess gene function in *V. inaequalis*.

The CRISPR-Cas9 system is a powerful tool for gene editing that has been established in many species of filamentous plant-pathogenic microbes. Indeed, CRISPR-Cas9 has been used to generate gene inactivations in more than 40 species of filamentous fungi and oomycetes (Schuster and Kahmann, 2019), including *Phytophthora sojae* (Fang and Tyler, 2016), *Magnaporthe oryzae* (Foster et al., 2018), *Ustilago maydis* (Schuster et al., 2016) and a fungus that is closely related to *V. inaequalis*, *Leptosphaeria maculans* (Idnurm et al., 2017). The CRISPR-Cas9 gene editing system requires two components: the Cas9 endonuclease and a single guide RNA (sgRNA). The Cas9 endonuclease is an RNA-guided enzyme that generates a double strand break (DSB) in the genome. The sgRNA often consists of a protospacer sequence of 20 nucleotides at the 5' end that targets specific DNA by base pairing, and an 80-nucleotide scaffold structure that binds to Cas9 (Krappmann, 2017). The sgRNA-Cas9 complex only cleaves the target DNA if it is flanked by a protospacer adjacent motif (PAM) (Doudna and Charpentier, 2014).

After the Cas9 endonuclease generates a DSB in the target DNA, DNA repair mechanisms of the target organism are activated (Doudna and Charpentier, 2014; Sander and Joung, 2014). The DNA can be repaired by a non-homologous end-joining mechanism (NHEJ) or homology-directed repair (HDR), although NHEJ is usually the dominant DNA repair pathway in fungi (Krappmann, 2007). DNA repair by NHEJ is error-prone and is likely to introduce small insertions/deletions (indels) or nucleotide substitutions, which can lead to frameshift mutations that cause a gene disruption (Sander and Joung, 2014). Alternatively, a double-stranded DNA template (donor DNA), usually harbouring a selectable marker, can be introduced to use as a repair template for HDR.

Traditionally, screening for the identification of mutants generated by the CRISPR-Cas9 system can be achieved using an enzymatic mismatch cleavage (EMC) method (Vouillot et al., 2015) or a polyacrylamide gel electrophoresis (PAGE)-based method (Zhu et al., 2014) that both rely on the detection of DNA heteroduplexes. Both EMC and PAGE detect large indels with a similar efficiency; however, the sensitivity with which they detect small indels (i.e. the type of indels that are usually generated following a CRISPR-Cas9 DSB) is low (Denbow et al., 2017; Vouillot et al., 2015; Zhu et al., 2014). Alternatively, CRISPR-Cas9 mutants can be identified by amplicon sequencing, which is a tedious and expensive process. A high-resolution melting (HRM) curve analysis is a fluorescence-based technique that measures the melting temperature of double-stranded DNA and, in doing so, can discriminate between amplicons with different melting temperatures (Reed and Wittwer, 2004; Simko, 2016; Wittwer, 2009). An HRM curve analysis has been widely used to identify mutations and single nucleotide polymorphisms in various genes (Dufresne et al., 2006; Reed and Wittwer, 2004), and has recently been used to reliably identify CRISPR-Cas9-mediated base pair (bp) indels in plants (Denbow et al., 2017; Li et al., 2020). To date, even though HRM curve analyses are largely used for fungal species identification, to our knowledge, an HRM curve analysis has not yet been employed to screen for CRISPR-Cas9-generated mutants in fungi.

In this study, we set out to establish the CRISPR-Cas9 gene editing system in *V. inaequalis*. For this purpose, we first generated the Golden Gate-compatible plasmid Cas9HygAMAccdB by modifying the previously published Cas9 autonomously replicating plasmid ANEp8-Cas9-LIC (Song et al., 2018). Here, Golden Gate-compatibility was chosen as it enabled the introduction of a sgRNA into Cas9HygAMAccdB using a single step, facilitating the creation of a Cas9HygAMA-*sgRNA* plasmid in less than one week. Next, using the melanin biosynthesis pathway gene *trihydroxynaphthalene reductase* (*THN*) as a proof of concept, we showed, in conjunction with the Cas9HygAMA-*sgRNA* plasmid, that the CRISPR-Cas9 gene editing system can be successfully applied to *V. inaequalis*. As part of this process, we also established a method based on an HRM curve analysis for the high-throughput screening of CRISPR-Cas9 gene-edited mutants of *V. inaequalis*.

2. Methods

2.1. Strains used and growth conditions

V. inaequalis isolate MNH120 from New Zealand (ICMP 13258; (Stehmann et al., 2001)) was used for CRISPR-Cas9 experiments, and was grown on a cellophane membrane (Waugh Rubber Bands) overlaying potato-dextrose agar (PDA) (Scharlab) at 22 °C with a 16 h light/8 h dark cycle. For long-term storage, *V. inaequalis* cellophane membranes were air-dried overnight and stored at −20 °C. *Escherichia coli* strain DH5α (Thermo Fisher Scientific) was used for cloning, propagation and maintenance of all plasmids without the *ccdB* gene, and *E. coli* strain TG1 (kindly provided by Jasna Rakonjac, Massey University) for propagation of all plasmids with the *control of cell death B* (*ccdB*) killer gene, in lysogeny broth (LB) at 37 °C and 180 rpm, or on LB agar at 37 °C.

2.2. Construction of the Cas9HygAMAccdB plasmid

The ANEp8-Cas9-LIC and ANEp8-Cas9-gRNA plasmids were kindly provided by Adrian Tsang from Concordia University. The first plasmid, ANEp8-Cas9-LIC, was previously constructed by Song et al. (2018) through the introduction of a 38-bp ligation-

independent cloning (LIC) site, centred with a *Swa*I restriction site, into the ANEp8-Cas9 plasmid. The second plasmid, ANEp8-Cas9-gRNA, was previously constructed by Song et al. (2018) through the introduction of a sgRNA cassette, via the LIC method, into the ANEp8-Cas9-LIC plasmid (see S5 Fig. of Song et al., [2018] for more details). We adapted the ANEp8-Cas9-LIC plasmid to contain a hygromycin resistance cassette in place of the *PyrG* gene for the selection of fungal transformants (summarized in Fig. S1A). To achieve this, the ANEp8-Cas9-LIC plasmid was first digested with *Not*I (New England Biolabs) to liberate a 5.3 Kb fragment containing the AMA1 cassette, and a 10.3 Kb fragment containing the *Cas9* and *PyrG* genes, with both fragments purified by gel extraction using a PureLink Quick Gel Extraction Kit (Thermo Fisher Scientific). Subsequent digestion of the 10.3 Kb fragment with *Kpn*I (New England Biolabs) liberated a 9 Kb Cas9 cassette containing the *Cas9* gene (i.e. through removal of the *PyrG* gene), which was again purified by gel extraction. Next, the 2.9 Kb hygromycin resistance cassette was amplified by PCR from pDONR221-Hyg (Fleetwood et al., 2007) using Phusion DNA polymerase (New England Biolabs), according to the manufacturer's instructions, in conjunction with the restriction enzyme-adapted primers *Not*I P*gpdA Hyg* pDONR Fw and *Kpn*I T*trpC Hyg* DONR Rv (Table 1), purified by gel extraction, and digested with both *Not*I and *Kpn*I. Following digestion, the *Not*I/*Kpn*I-digested Cas9 cassette and the *Not*I/*Kpn*I-digested hygromycin resistance cassette were ligated together with T4 ligase (Invitrogen) at 16 °C overnight to create the Cas9Hyg plasmid, and then purified using a PureLink Quick Plasmid Miniprep Kit (Invitrogen). Finally, the Cas9Hyg plasmid was digested with *Not*I, dephosphorylated with Shrimp Alkaline Phosphatase (rSAP) (New England Biolabs), and purified by gel extraction, before ligation with the *Not*I-digested AMA1 cassette using T4 ligase to create the Cas9HygAMA plasmid.

Next, we set out to create the CasHygAMASapI plasmid by adding the sgRNA cassette, which contains a mock 20-bp sgRNA protospacer flanked by *Sap*I restriction sites, to the Cas9HygAMA plasmid (summarized in Fig. S1A). This was achieved through overlap fusion PCR and LIC (Song et al., 2018). More specifically, a fragment containing the tRNA promoter and mock protospacer sequences was first amplified from the ANEp8-Cas9-gRNA plasmid by PCR, as above, using the primers Fw LIC2 and *Sap*I site CRISPR Rv (Table 1). Here, the *Sap*I site CRISPR Rv primer was designed to introduce a *Sap*I restriction site between the tRNA promoter and mock protospacer sequences. At the same time, a second fragment containing the mock protospacer and tRNA terminator sequences was amplified from the ANEp8-Cas9-gRNA plasmid by PCR using the primers *Sap*I site CRISPR Fw and Rv LIC2 (Table 1). In this case, the *Sap*I site CRISPR Rv primer was designed to introduce a *Sap*I restriction site between the mock protospacer and tRNA terminator sequences. Following gel extraction, the two purified fragments were then fused by PCR. For this purpose, 1 ng of each of the purified PCR fragments was combined and used as template in a 25 μL PCR with Phusion DNA polymerase in conjunction with the Fw LIC2 and Rv LIC2 primers (Table 1). The overlap fusion PCR was performed with the following thermocycler program: 30 s at 98 °C, followed by 35 cycles of 98 °C for 5 s, 60 °C for 10 s, 72 °C for 30 s, and then a final step of 72 °C for 10 min. Finally, upon gel extraction, the purified PCR product was inserted into the Cas9HygAMA plasmid through LIC via its *Swa*I restriction site (Song et al., 2018) to create the Cas9HygAMASapI plasmid.

Lastly, to insert the *ccdB* and *chloramphenicol acetyltransferase* (*cat*) resistance genes into the Cas9HygAMASapI plasmid (i.e. for subsequent cloning and screening), a 2 Kb fragment containing the *ccdB* and *cat* resistance gene cassette was amplified by PCR, as above, from pSM1 (Rahnama et al., 2017) using the *Sap*I restriction enzyme-adapted primers *Sap*I *ccdB* Fw and *Sap*I *ccdB* Rv (Table 1). The resulting product was purified by gel extraction, digested by *Sap*I at 37 C, and ligated into the *Sap*I-digested Cas9HygAMASapI

Table 1
Oligonucleotides used in this study. Bold sequence corresponds to the *Sap*I restriction site. Italicised sequence corresponds to the *Not*I restriction site. Bold italicized sequence corresponds to the *Kpn*I restriction site.

Oligonucleotide name	Oligonucleotide sequence (5′–3′)
MR135	**GTC**TTTCAAGGACGTCACACCAG
MR136	**AAC**CTGGTGTGACGTCCTTGAAA
MR137	**GTC**GCCCCATCATGGTCTTTGGA
MR138	**AAC**TCCAAAGACCATGATGGGGC
MR139	TTTTCTCTTCCATTTACGC
MR161	GTAGGGAGGTCCATTAGTG
MR162	GGATAACACACTAGAGATA
MR170	TTATAGTCGACCACCGCTCG
MR171	CCACGACCTGTTGATTGCAT
MR172	CCCACTCACTAAACAAACTA
MR173	TCGATTGACAAGAACATACC
MR182	GCATCTGACGCCCCATCATGGGGTTT
MR183	AAACCCCATGATGGGGCGTCAGATGC
MR184	GCGAGAATGCAGAGAGTTGG
MR185	GTGTGTGTCGCTGGATGATC
MR204	CGCCAGCCTTCAATGCCAAT
MR205	CATTGCGCCATCCCGATCTG
MR252	CGTTGGCCAATCAGACGTCG
MR253	GCCCAGAGCATCATCACCCT
MR258	GAGCGGATTCCTCAGTCTCG
MR259	CTCGGAGGGCGAAGAATCTC
*Kpn*I T*trpC Hyg* DONR Rv	GCC***GGTACC***GCGCTTACACAGTACACGAG
*Not*I P*gpdA Hyg* pDONR Fw	AAGGAAAAAAA*GCGGCCGC*CTAAAATCCGCCGCCTCCAC
*Sap*I site CRISPR Fw	GTCGGAAGAGCAAAAT**GCTCTTC**AGTTTTAGAGCTAGAAATAGCAAG
*Sap*I site CRISPR Rv	AACTGAAGAGCATTTT**GCTCTTC**CGACGAGCTTACTCGTTTCG
Fw LIC2	CAACCTCCAATCCAATTTGACTCCGCCGAACGTACTGG
Rv LIC2	ACTACTCTACCACTATTTGAAAAGCAAAAAAGGAAGGTACAAAAAAGC
*Sap*I *ccdB* Fw	TCGGCTCGTCGGAAGAGCGACCGACAGCCTTCCAAATG
*Sap*I *ccdB* Rv	TCGCTAAAACTGAAGAGCGTTGGCAGCATCACCCGACG

plasmid using T4 ligase at 16 °C for 24 h to create the Cas9HygAMAccdB plasmid (Fig. 1 and Supplementary Information 1).

2.3. Protospacer design and cloning

The *V. inaequalis THN* gene (Joint Genome Institute ID: *atg4736.t1*) was screened for CRISPR-Cas9 target sites with the PAM (NGG) sequence using the 'Find CRISPR Sites' function in Geneious (v.9.0.5) (Kearse et al., 2012). Only those protospacers with no predicted off-target effects (i.e. a Specificity score of 100%), an on-target (Activity) score of at least 0.4, and no predicted off-target binding sites in the *V. inaequalis* MNH120 PacBio reference genome (unpublished, The New Zealand Institute for Plant and Food Research Limited) using BLASTn, were considered. Based on these criteria, two protospacer sequences with the best on-target score, targeting the first and second exon of the *THN* gene, respectively, were selected. Each protospacer, with the appropriate *Sap*I overhang for Golden Gate cloning into the destination plasmid Cas9HygAMAccdB, was ordered as a forward and reverse oligonucleotide from Integrated DNA Technologies. The protospacer #20 was generated by pre-annealing 40 ng of the forward (MR135) and reverse (MR136) oligonucleotides (Table 1), and protospacer #4 by pre-annealing 40 ng of the forward (MR137) and reverse (MR138) oligonucleotides (Table 1), in annealing buffer (10 mM Tris–HCl pH 8, 50 mM NaCl, 1 mM EDTA, pH 8) with the following thermocycler program: 5 min at 95 °C, 20 s at 92 °C, followed by a decrease of 0.5 °C each cycle for 140 cycles, and finally, 1 min at 25 °C. Pre-annealed oligonucleotides were cloned into the Cas9HygAMAccdB plasmid using Golden Gate in association with the *Sap*I restriction enzyme to generate sgRNA20 and sgRNA4. Golden Gate reactions were performed with the following thermocycler program: 1 min at 37 °C, 1 min at 16 °C for 30 cycles, followed by 5 min at 55 °C and 5 min at 80 °C. Transformants positive for each Cas9HygAMA-*sgRNA* plasmid were screened by colony PCR using Taq DNA polymerase (New England Biolabs) with the forward Cas9HygAMAccdB primer (MR139) and reverse sgRNA-specific primer (MR136 or MR138) (Table 1). Colony PCRs were carried out with the standard manufacturer's protocol. Sequence authenticity of the sgRNAs was confirmed by PCR amplicon sequencing, provided by the Massey Genome Service (Massey University, Palmerston North, New Zealand), using the MR139 forward Cas9HygAMAccdB primer.

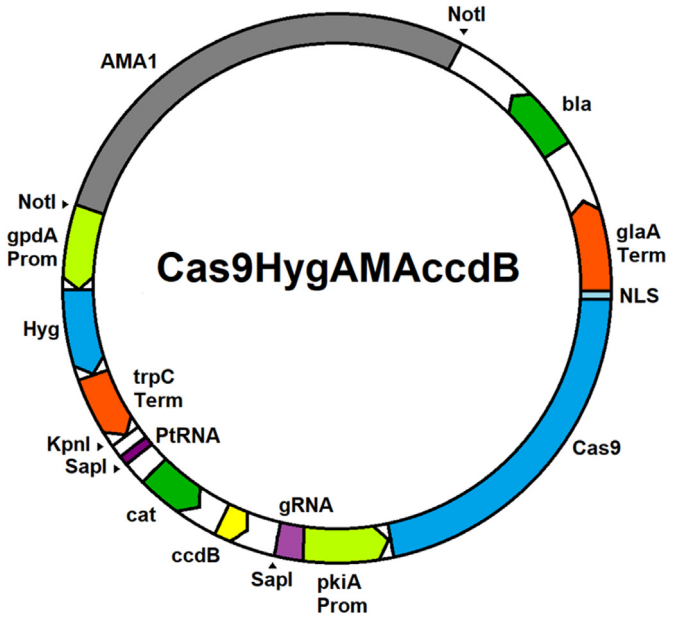

Fig. 1. Schematic representation of the Cas9HygAMAccdB plasmid. The plasmid, which is 19,273 bp in size, contains the autonomously replicating sequence AMA1 from *Aspergillus nidulans*, as well as the *cas9* gene from *Streptococcus pyogenes* (codon-optimized based on *Asergillus niger*), which is flanked by the *A. niger* pyruvate kinase gene promoter (*pkiA* Prom) and the *A. niger* glucoamylase gene terminator (*glaA* Term) (Song et al., 2018). Fused to the carboxyl (C)-terminus of the *cas9* gene is a nucleotide sequence encoding a nuclear localization signal (NLS). The Cas9HygAMAccdB plasmid also contains a hygromycin B resistance casette (Hyg) flanked by the *A. nidulans* glyceraldehyde-3-phosphate dehydrogenase gene promoter (*gpdA* Prom) and the *A. nidulans* tryptophan C gene terminator (*trpC* Term) (Fleetwood et al., 2007). *Sap*I restriction sites for introduction of a sgRNA cassette by Golden Gate cloning (i.e. through replacement the control of cell death B [*ccdB*] gene) are shown. *bla*: beta-lactamase gene conferring ampicillin resistance; *cat*: chloramphenicol acetyltransferase gene conferring chloramphenicol resistance.

3. *V. inaequalis* protoplast preparation and transformation

Cas9HygAMA-*sgRNA* plasmids were introduced into *V. inaequalis* using a PEG-mediated protoplast transformation protocol. For this purpose, *V. inaequalis* was first grown on cellophane membranes overlaying PDA for 10–14 days. Fungal mycelia on top and inside cellophane membranes were then macerated in 1.5 ml microcentrifuge tubes using plastic micropestles, transferred to a 250 ml Erlenmeyer flask containing 30 ml potato-dextrose broth (PDB) (Difco), and cultured without shaking in the dark at 22 °C for 48 h. After culturing, fungal material was harvested by centrifugation at 2,800 *g* for 20 min, washed three times with KC buffer (0.60 M KCl, 50 mM $CaCl_2 \cdot 2H_20$), with collection by centrifugation as above after each wash, and incubated in a 250 ml Erlenmeyer flask containing 10 g/L *Trichoderma harzianum* lysing enzymes (Sigma–Aldrich) in 50 mL kC buffer at 24 °C and 80 rpm for 4–5 h. Finally, protoplasts were filtered through glass wool, and washed three times with KC buffer as above. Protoplasts were counted using a haemocytometer and re-suspended to a final concentration of 10^4–10^5 protoplasts/ml.

Transformation was performed by mixing 100 µl of *V. inaequalis* protoplasts (10^4-10^5 protoplasts/ml) with 100 µl of 25% PEG4000, 10 µg of circular Cas9HygAMA-*sgRNA* plasmid DNA, and 5 µl of 50 µM sterile spermidine. The protoplast-PEG mixture was then chilled on ice for 20 min and 500 µl of 25% PEG4000 gently added. Each protoplast-PEG mixture was plated across five Sucrose Hepes (SH) plates (0.6 M sucrose, 5 mM HEPES, 0.6% agar) and incubated at 20 °C for 48 h. After incubation, protoplasts were overlaid with ½-strength PDA cooled-down to ~50 °C and supplemented with 50 mg/ml hygromycin B (Merck). Transformants appearing on the PDA surface, between two and three weeks after transformation, were transferred to 16-well PDA plates supplemented with 50 mg/ml hygromycin B, and grown until abundantly sporulating. After mutant screening, selected transformants were single-spore-purified. This was achieved by re-suspending a single colony in 500 µl sterile water and vortexing for 30 s, with 100 µl streaked onto 4% water agar (WA) plates and the conidia germinated for 24 h. Following germination, one single germinated conidium was transferred to a cellophane membrane overlaying PDA for continued growth.

3.1. V. inaequalis *genomic DNA extraction*

Two-to-four week-old cultures of *V. inaequalis* grown on cellophane membranes were freeze-dried and ground to a fine powder in liquid nitrogen with a pre-cooled mortar and pestle, and approximately 300 mg of powder was transferred to a 1.5 ml microcentrifuge tube. To this, 1 ml of DNA extraction buffer (0.5 M NaCl, 10 mM Tris–HCl, 10 mM EDTA, 1% SDS, pH 7.5) was added, vortexed, and incubated at 65 °C for 30 min, followed by 2 min incubation at room temperature (RT). Fungal material was collected

by centrifugation at 16,000 *g* for 2 min and 800 μl of supernatant was transferred to a fresh 1.5 ml microcentrifuge tube. Then, 4 μl of RNase A (20 mg/ml) (Invitrogen) was added and samples were incubated at 37 °C for 15 min. After incubation, a 0.5 volume of phenol and a 0.5 volume of chloroform:isoamyl alcohol (24:1) were added and samples were centrifuged for 5 min at 16,000 *g*. The aqueous phase was then transferred to a fresh 1.5 ml microcentrifuge tube and 1 volume of phenol:chloroform (1:1) was added. Samples were again centrifuged at 16,000 *g* for 5 min and the supernatant transferred to a new 1.5 ml microcentrifuge tube. The chloroform:isoamyl alcohol (24:1) step was then repeated and the supernatant was transferred to a new 1.5 ml microcentrifuge tube. Genomic DNA was precipitated by the addition of a 0.1 volume of 3 M sodium acetate (pH 5.2) and two volumes of 95% ethanol. Samples were mixed by inversion and incubated overnight at −20 °C. Following incubation, the precipitated DNA was collected by centrifugation at 16,000 *g* for 30 min, and the supernatant was decanted. The genomic DNA pellet was then washed with 200 μl of 70% ethanol and collected by centrifugation at 16,000 *g* for 5 min. Finally, the genomic DNA pellet was air-dried for 15–30 min and suspended in 50 μl of MilliQ water.

3.2. High resolution melting curve analysis

A positive control for the HRM curve analysis was created by site-directed mutagenesis. First, primers MR161 and MR162 (Table 1) were phosphorylated with T4 Polynucleotide Kinase (New England Biolabs) at 37 °C for 1 h in a 4.5 μl reaction volume with 10 μM primer, 10x T4 ligase buffer (New England Biolabs) and 0.4 μl of T4 polynucleotide kinase (New England Biolabs). The *THN* gene was amplified with the phosphorylated primers MR161 and MR162 using Phusion Flash High-Fidelity PCR Master Mix (Thermo Fisher Scientific) and purified using an OMEGA Gel Extraction kit. pICH41021 (kindly provided by Dr Kee Hoon Sohn, formerly of Massey University) was digested with the *Sma*I restriction enzyme in a 50 μl volume for 2 h at 37 °C. Digested plasmid was then dephosphorylated with rSAP for 30 min at 37 °C, with the reaction subsequently heat-inactivated at 65 °C for 5 min. Finally, the *THN* gene was ligated to pICH41021 in a 3:1 M ratio using T4 Ligase (New England Biolabs) at 4 °C overnight and transformed by heat shock into chemically competent *E. coli* cells. Positive transformants were confirmed by colony PCR. Next, the pICH41021-*THN* plasmid was amplified with overlapping primers MR182 and MR183 to introduce a mutation in the *THN* gene that substituted a thymine and cytosine at nucleotide positions 26 and 27 for two guanines. Authenticity of the resulting re-circularized pICH41021-$THN_{TC(26/27)GG}$ DNA was confirmed by sequencing.

Two sets of primers (MR170-MR171 and MR172-MR173) were designed with Geneious v.9.0.5 software for use in the HRM curve analysis (Table 1). These primers were designed to amplify the DNA region in the *THN* gene recognized by the sgRNA (and thus, edited by the Cas9 endonuclease), with an amplicon size of 123 bp (MR172-MR173) and 230 bp (MR170-MR171). Primers were tested to be specific and suitable for HRM by performing an HRM curve analysis with DNA standards (wild-type and engineered positive control), as described below, with the resulting amplicons resolved by electrophoresis on a 1.5% Tris-acetate-EDTA (TAE) gel.

The HRM curve analysis was performed using a LightCycler 480 Instrument (Roche) with the AccuMelt HRM SuperMix fluorescent dye (DNAture) in a 20 μL reaction with 1x AccuMelt HRM SuperMix, 300 nM forward primer (MR172), 300 nM reverse primer (MR173) and 1.5 ng of genomic DNA template or 0.01 ng of pICH41021-$THN_{TC(26/27)GG}$. At least two technical replicates were performed for each sample. The qPCR amplification was performed with the following program: initial denaturation of 5 min at 95 °C, followed by 40 cycles of 95 °C for 8 s, 60 °C for 15 s, 70 °C for 20 s, with one fluorescence reading per annealing step. The qPCR was followed by a melting program consisting of 95 °C for 1 min, 40 °C for 1 min and 76 °C for 1 s, at which point the temperature was ramped up to 92 °C (with a temperature increase of 0.02 °C per second, and a continuous signal acquisition mode made up of 25 acquisitions per degree), followed by a cooling step of 40 °C for 30 s. The HRM curve data were analysed with the LightCycler 480 gene scanning software. To confirm mutants identified by HRM, the *THN* gene was amplified with Phusion Flash High-Fidelity PCR Master Mix using primers MR161 and MR162, with the resultant PCR amplicons gel-purified as above and sequenced using primer MR161.

3.3. Southern blot analysis

For the detection of Cas9HygAMAccdB-*sgRNA* plasmid DNA in genomic DNA samples of *V. inaequalis* by Southern blotting, a probe binding to the hygromycin resistance cassette of the Cas9HygAMAccdB plasmid was generated by PCR using Phusion DNA polymerase in conjunction with primers MR258 and MR259 (Table 1), purified by gel extraction, and labelled with digoxigenin (DIG) using a High Prime DNA Labelling and Detection Starter Kit I (Roche) according to manufacturer's instructions. Genomic DNA was then extracted from wild-type *V. inaequalis*, as well as single-spore-purified transformants of *V. inaequalis*, using the method described in section 3.1. A total of 5 μg genomic DNA from each sample, as well as 50 ng of Cas9HygAMAccdB plasmid DNA (positive control DNA), was subsequently digested with the *Eco*RI restriction enzyme (New England Biolabs) overnight at 37 °C and resolved by electrophoresis on a 1.5% Tris-borate-EDTA (TBE) gel. Following electrophoresis, DNA was transferred to a positively charged nylon membrane (Roche) overnight at RT. DNA was crosslinked to the membrane by UV irradiation for 2 min using a CEX-800 UV cross-linker (120 mJ/cm2, 254 nm; Ultralum, Inc.), and the probe hybridized to the DNA on the membrane overnight at 50 °C. Colorimetric detection of the probe was then performed as per the manufacturer's instructions using the DIG High Prime DNA Labelling and Detection Starter Kit I for 3 h for the Cas9HygAMAccdB plasmid DNA control, and 9 h for *V. inaequalis* genomic DNA samples.

4. Results and discussion

4.1. CRISPR-Cas9 can be used for gene disruption in V. inaequalis

We set out to establish the CRISPR-Cas9 gene editing system in *V. inaequalis*, using the melanin biosynthesis pathway gene *THN* (Joint Genome Institute ID: *atg4736.t1*) as a target for inactivation. The *THN* gene was chosen as a proof of concept, as a previous study had shown that *V. inaequalis* displays a distinctive light-brown phenotype when this gene is transcriptionally silenced using RNAi, indicative of reduced melanisation (Fitzgerald et al., 2004). In this way, transformants of *V. inaequalis* inactivated for the *THN* gene using the CRISPR-Cas9 gene editing system can be rapidly identified through a simple visual screen. For ease of use, we chose to employ a CRISPR-Cas9 gene editing system that, similar to the one previously established in *Aspergillus niger* (Song et al., 2018), only requires a single autonomously replicating plasmid (derived from Cas9HygAMAccdB, and containing both the Cas9 endonuclease and sgRNA) for gene inactivation (Fig. 1).

The Cas9HygAMAccdB plasmid contains an *A. niger* codon-optimized *cas9* gene expressed under the control of the *pkiA* (*pyruvate kinase*) promoter. To ensure expression in the fungal nucleus, the Cas9 endonuclease was tagged at its carboxyl (C) terminus with a nuclear localization signal (NLS). The Cas9HygAMAccdB plasmid

also contains an RNA polymerase III promoter to facilitate expression of the sgRNA *in vivo*. Using the chosen CRISPR-Cas9 system, the 20 bp encoding the sgRNA protospacer were synthesized as two pairs of complementary oligonucleotides that were pre-annealed and cloned into the Cas9HygAMAccdB plasmid by a single-step Golden Gate reaction, enabling Polymerase Chain Reaction (PCR)-free cloning that could be completed in less than one week.

An autonomously replicating plasmid was chosen as it has several advantages. Firstly, autonomously replicating plasmids can enhance fungal transformation efficiency, as recombination between the plasmid and chromosome is not required (Aleksenko and Clutterbuck, 1997). As such, autonomously replicating plasmids can be used in fungal species that exhibit low transformation efficiency, such as *V. inaequalis*. Secondly, autonomously replicating plasmids could be lost once selection (e.g., as mediated through hygromycin B) is removed (Aleksenko and Clutterbuck, 1997). In doing so, autonomously replicating plasmids can reduce off-target effects by only enabling transient expression of the Cas9 endonuclease in the fungus (Nødvig et al., 2015). As such, autonomously replicating plasmids could be recycled, which would enable the sequential inactivation of genes in CRISPR-Cas9 gene-edited mutants and could also facilitate the subsequent complementation of mutants generated using CRISPR-Cas9 technology.

As a starting point for inactivation, sgRNAs were designed to target the amino (N) terminus (first and second exon) instead of the C terminus of the *THN* gene. This is because mutations at the C terminus of a gene are less likely to cause a frameshift mutation that results in inactivation (Doench et al., 2014). As different sgRNAs can display different targeting efficiencies (Doench et al., 2014), two different sgRNAs, sgRNA 4 and sgRNA 20, with similar predicted on-target activity, and no predicted off-target activity (Table 2), were selected for inactivation of the *THN* gene. Special attention was taken to ensure that the sgRNAs did not target any other melanin biosynthesis pathway genes that have a high degree of conservation to *THN*, such as the *1,3,6,8-tetrahydroxynaphthalene reductase* gene (*atg3631.t1*). PEG-mediated protoplast transformation of *V. inaequalis* with sgRNA 4, targeting the first *THN* exon (Fig. 2A), resulted in 98 independent transformants, of which 62 ceased to grow on hygromycin B selection media after one week, and were therefore considered transient, giving a final number of 36 stable transformants. Transient transformants have been reported in a large number of PEG-mediated protoplast transformations of fungi (Hamada et al., 1994; Sánchez-Torres et al., 1994), and it has previously been reported that up to 98% of PEG-mediated protoplast transformants of *V. inaequalis* are transient (Fitzgerald et al., 2003). Of course, it remains possible that the large number of transient transformants generated in our study was the result of premature loss of the autonomously replicating plasmid used to deliver the sgRNA and Cas9.

Notably, of the 36 stable transformants, six had a light-brown phenotype (Fig. 2B). These were transformants THN #9, THN #37, THN #60, THN #66, THN #89 and THN #96. To validate the presence of a mutation in the *THN* gene, it was amplified from each of the six putative mutants by PCR, as well as from three dark-brown transformants without the light-brown phenotype (THN #38, THN #53 and THN #90), and subjected to amplicon sequencing. As expected, all three dark-brown transformants did not contain a mutation in their *THN* gene (Fig. 2C). For the putative light-brown mutant THN #9, the *THN* gene could not be amplified by PCR using two different sets of primers (MR161-MR162, MR185-MR186). This was despite the fact that both *THN*-flanking genes could be amplified, suggesting that a large deletion at the *THN* locus might have occurred (Fig. S2). In contrast to the dark-brown transformants, the remaining light-brown *THN* transformants displayed a range of mutations. More specifically, these were a single bp insertion (T) at the same location in THN #37 and THN #66, a 33-bp deletion (TTTGGAGGGCAAGGTCGCCCTCGTTACCGGTTC) in THN #60, a single bp deletion (T) in THN #89, and a 24-bp deletion (TCATGGTCTTTGGAGGGCAAGGTC) in THN #96. Therefore, from the 36 stable transformants, six had a confirmed mutation, giving a gene inactivation efficiency of ~16.7%.

CRISPR-Cas9 gene inactivation efficiencies in other filamentous fungi, in experiments that rely on NHEJ, range between 10 and 100% (DiCarlo et al., 2013; Foster et al., 2018; Khan et al., 2020; Schuster et al., 2016; Shi et al., 2017). In cases where the CRISPR-Cas9 NHEJ-based gene inactivation efficiency is low, the gene inactivation efficiency could be improved greatly by the incorporation of a donor DNA that is integrated into the genome using HDR (Foster et al., 2018). Nevertheless, gene inactivation efficiencies between experiments cannot be compared, as these efficiencies will greatly depend on Cas9 expression, sgRNA design and accessibility of the target gene, among other factors (Schuster and Kahmann, 2019). Therefore, even though the inactivation efficiency of the *V. inaequalis THN* gene with sgRNA 4 is at the low end, it is likely to vary between genes and no conclusions can yet be drawn as to the overall efficiency of the technique.

Remarkably, PEG-mediated protoplast transformation of *V. inaequalis* with sgRNA 20, targeting the second exon of the *THN* gene (Fig. 2A), resulted in a similar number of stable independent transformants on hygromycin B selection media (31 in total), but none of these transformants had the distinctive light-brown phenotype, indicating that if a Cas9-induced mutation was generated, it was synonymous or did not disrupt THN activity. This stark difference in the number of transformants inactivated for the *THN* gene is interesting, given that both sgRNAs had a similar predicted on-target activity score (Table 2). However, it is known that different sgRNAs can vary greatly in their efficiency, as previously observed for sgRNAs targeting the *yA* gene of the filamentous fungus *Aspergillus nidulans* (Nødvig et al., 2018), highlighting the importance of reliable methods to estimate sgRNA efficiency. Thus, while genes will differ in their ability to be inactivated using the CRISPR-Cas9 gene editing system (e.g. due to their location in the genome) (Schuster and Kahmann, 2019), it is important that future studies consider multiple sgRNAs for successful gene inactivation in *V. inaequalis*.

Table 2
Selected sgRNA protospacers used to target the *Venturia inaequalis* melanin biosynthesis pathway gene *trihydroxynaphthalene reductase* (*THN*).

	Sequence (5′–3′)[a]	Binding site	Direction	Off-targets[b]	Off-target score[c]	On-target score[d]
Protospacer 4	GCCCCATCATGGTCTTTGGAGGG	Exon 1	Forward	0 (0 in CDS)	100%	0.448
Protospacer 20	TTTCAAGGACGTCACACCAGAGG	Exon 2	Forward	0 (0 in CDS)	100%	0.539

[a] NGG: protospacer adjacent motif (PAM) site.
[b] CDS: coding sequence.
[c] Off-target score: prediction of how likely a sgRNA sequence might bind to somewhere else in the genome. Scores are between 0 and 100, with higher scores indicative of less off-target activity.
[d] On-target scores are between 0 and 1, with higher scores indicative of higher expected activity of the sgRNA-Cas9 complex on the target gene, based on Doench et al. (2014).

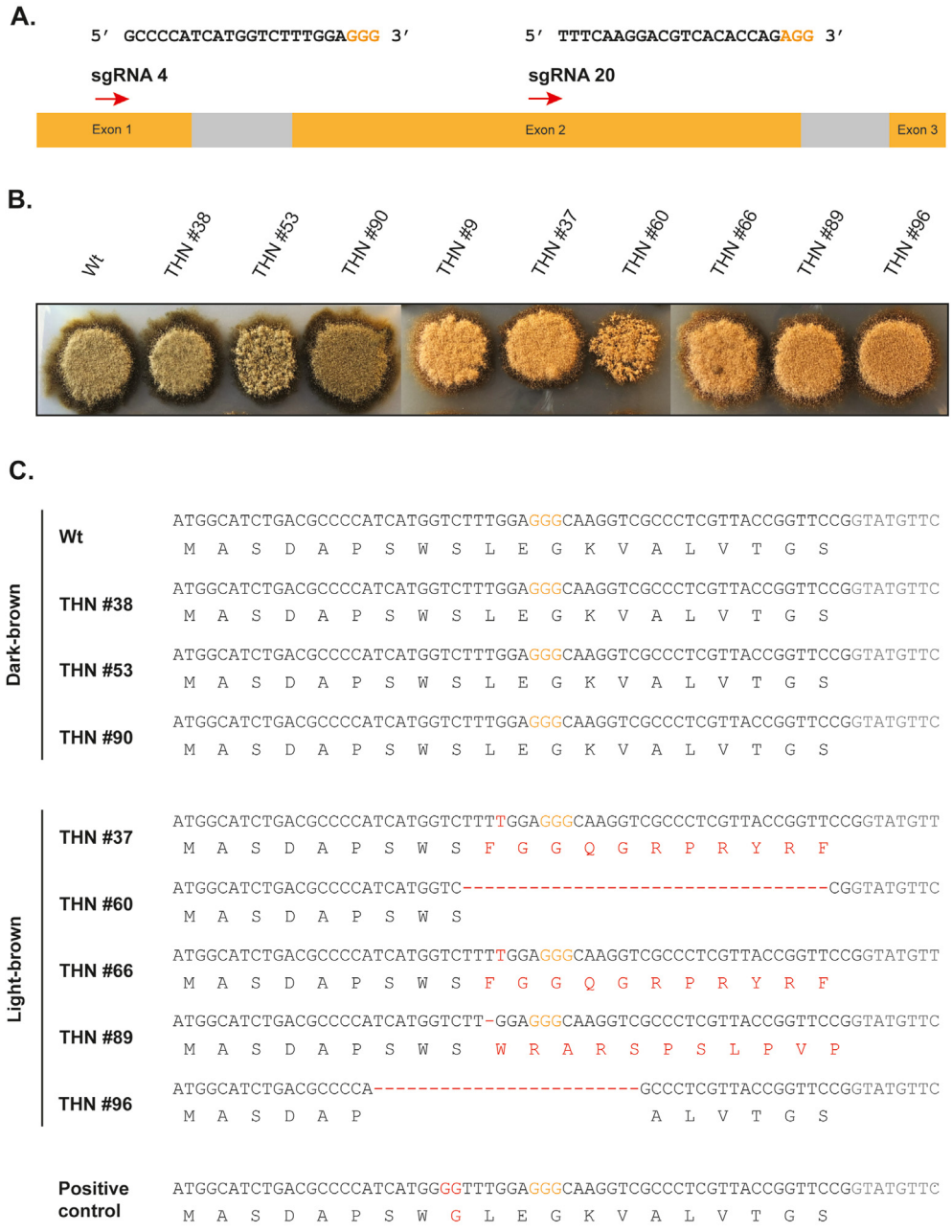

Fig. 2. Establishment of the CRISPR-Cas9 gene editing system in *Venturia inaequalis*. **A.** Schematic representation of the *V. inaequalis* melanin biosynthesis pathway gene *trihydroxynaphthalene reductase* (*THN*; 911 bp) with binding sites for the two selected sgRNAs used in CRISPR-Cas9 gene editing experiments shown. Orange: gene exons; Grey: gene introns; Bold nucleotides: expected sgRNA cleavage site; orange nucleotides: PAM site. Arrows: binding direction of sgRNAs. **B.** Colony phenotype of wild type (wt) *V. inaequalis*, and three dark-brown and six light-brown CRISPR-Cas9 transformants grown on potato-dextrose agar at 22 °C for 14 days. **C.** Spectrum of CRISPR-Cas9-generated mutations in the *THN* gene. Black nucleotides: exon; Grey nucleotides: intron; Orange nucleotides: PAM site; Red amino acids/nucleotides: mutations observed. Light-brown mutant THN #9 was not sequenced due to a lack of PCR amplification for the *THN* gene. (For interpretation of the references to color in this figure legend, the reader is referred to the Web version of this article.)

4.2. The autonomously replicating CRISPR-Cas9 gene editing plasmid is rapidly lost in most transformants once selection is removed

With the finding that the CRISPR-Cas9 gene editing system could be successfully applied to *V. inaequalis*, we next set out to determine whether this fungus can lose the autonomously replicating plasmid, Cas9HygAMA-*sgRNA*, once the hygromycin B selection is removed. For this purpose, all six light-brown *THN* mutants (THN #9, THN #37, THN #60, THN #66, THN #89 and THN #96), as well as three dark-brown transformants (THN #38, THN #53 and THN #90), all derived from the transformation of *V. inaequalis* with sgRNA 4, were single-spore-purified and replica-plated onto both PDA and PDA supplemented with 50 μg/ml hygromycin B. After only one round of single-spore isolation and sub-culturing, four of the *THN* mutants (THN #60, THN #66, THN #89 and THN #96) and two of the transformants without the light-brown phenotype (THN #53 and THN #90) lost the ability to grow on PDA supplemented with hygromycin B, suggesting that they have lost the Cas9HygAMA-*sgRNA* plasmid (Fig. S3).

To confirm that this is indeed the case, and to assess whether the remaining transformant (THN #38) and *THN* mutants (THN #9 and THN #37) still possess the Cas9HygAMA plasmid in its autonomously replicating form, or whether this plasmid has instead been integrated into their genomes, a Southern blot experiment was performed using a probe binding to the hygromycin B cassette of the Cas9HygAMA plasmid (Fig. S4). Here, genomic DNA from each of the transformants and *THN* mutants was digested with the restriction enzyme *Eco*RI. Similar amounts of *Eco*RI-digested genomic DNA from each of the transformants and THN mutants was used for Southern blot as observed by gel electrophoresis prior to membrane transfer and blotting (Fig.S4A). For the *THN* mutant THN #37, two bands of approximately 2.7 Kb and 2.4 Kb, respectively, corresponding to the expected banding profile of *Eco*RI-digested Cas9HygAMA plasmid DNA, were observed, indicating that the autonomously replicating plasmid was still present (Fig. S4B). However, in addition to these two bands, several bands ranging in size from approximately 3.2 Kb to >10 Kb that do not correspond to the expected banding profile of *Eco*RI-digested Cas9HygAMA plasmid DNA, were also observed (Fig. S4B). This suggests that multiple integrations of Cas9HygAMA plasmid DNA into the genome of *THN* mutant THN #37 have also occurred. Unlike THN #37, the *THN* mutants THN #9 and THN #38 were only found to have unique bands that do not correspond to the autonomously replicating Cas9HygAMA plasmid (Fig. S4B). This suggests that these transformants do not possess the plasmid in its autonomously replicating form, but rather, that it has integrated into their genomes. Finally, the Cas9HygAMA plasmid, either in its autonomously replicating form or as a version that has been integrated into the genome, could not be detected in transformants THN #53 and THN #90, as well as *THN* mutants THN #60, THN #66, THN #89 and THN #96 (Fig. S4B), which collectively lost the ability to grow on PDA supplemented with hygromycin B (Fig. S3), confirming that they have indeed lost the autonomously replicating Cas9HygAMA plasmid (Fig. S4B).

4.3. *High-resolution melting analysis is a sensitive and high-throughput method to screen for CRISPR-Cas9 mutants*

In our study, mutants of *V. inaequalis* with a CRISPR-Cas9-mediated gene inactivation of the *THN* gene could be rapidly identified based on their light-brown colony phenotype. However, not all genes of *V. inaequalis* will result in an observable phenotype when inactivated or mutated. For this reason, a low-cost, high-throughput method is required to rapidly identify CRISPR-Cas9 gene-edited mutants of *V. inaequalis* that lack an observable phenotype on a transformation plate facilitating selection. One such method is an HRM curve analysis, which enables the rapid identification of single bp indels in DNA amplicons from transformant genomic DNA (Reed and Wittwer, 2004; Simko, 2016; Wittwer, 2009). We set out to test the efficiency of an HRM curve analysis for the detection of *V. inaequalis THN* mutants generated using CRISPR-Cas9 sgRNA 4. As a starting point for this analysis, we first generated a positive control sequence for detecting indels relative to the wild type (wt) sequence (Fig. 2C). The positive control was generated by introducing a two-nucleotide substitution into a PCR amplicon of the *THN* gene using site-directed mutagenesis.

According to the literature, an HRM curve analysis can be affected by different parameters such as genomic DNA quality, PCR amplicon size, amplicon GC content and fluorescent dye used (Słomka et al., 2017). To ensure reliability of the assay, good quality genomic DNA should be extracted. Likewise, the same DNA preparation method should be used across all samples to ensure uniformity in genomic DNA quality. Amplicon size is another crucial parameter that affects the HRM curve analysis. Therefore, two different primer sets were designed to generate amplicons of 230 bp (MR170-MR171) and 123 bp (MR172-MR173) (Table 1). The HRM curve assay was performed with both primers sets using wt genomic DNA and the engineered positive control as DNA template. Specific DNA amplicons could be amplified using both primers sets (Fig. 3A); however, the smaller amplicon showed a clearer shift in the melting curve between wt and positive control (Fig. 3B). Given that smaller amplicons are more suitable for HRM curve analysis (Słomka et al., 2017), and because the smaller amplicon showed a clearer shift in the melting curve, we decided to use the 123 bp amplicon for our screen (primer set MR172-MR173).

The HRM curve analysis was performed using the AccuMelt HRM SuperMix high saturating dye SYTO 9™, resulting in clear separation of unique melting curves between mutants (Fig. 4). The normalized HRM curves showed that amplicons from wt fungus, as well as dark-brown transformants, clustered together into a group with a similar melting curve profile (blue curves in Fig. 4). In contrast, amplicons from the engineered positive control (green curves in Fig. 4) and the light-brown *THN* mutants showed distinct melting curves (green, red, grey and purple curves in Fig. 4) that correlated with the different mutations seen in Fig. 2C. These results indicate that the HRM curve assay can not only efficiently identify CRISPR-Cas9 gene-edited mutants, but can also discriminate between different types of mutations (Reed and Wittwer, 2004). The light-brown mutant THN #9 could not be screened using the HRM curve analysis due to a lack of PCR amplification for the *THN* gene, suggesting that a large deletion at the *THN* locus has been generated. This highlights one of the main limitations of the HRM curve analysis, in that it is not suitable for the detection of large deletion mutants. However, given that such deletion mutants can be easily assessed using standard PCR, this is not an issue.

One of the main advantages of the HRM curve analysis is that it can detect mutant DNA that is mixed in with wt DNA, even when the amount of mutant DNA is as low as 1–5% (Denbow et al., 2017; Li et al., 2020). To test the efficiency of the HRM curve assay, genomic DNA from one mutant with a single bp insertion (THN #66) was mixed with wt genomic DNA at different mutant:wt ratios (1:99, 5:95, 10:90, 20:80, 30:70 and 50:50), similarly to that performed by (Denbow et al., 2017). Under our conditions, the assay could not differentiate mutant and wt in 1:99 mutant:wt ratio; however, the mutant DNA could be identified by the HRM curve analysis in all of the other ratios, with a clear shift in the melting curve, indicating an assay sensitivity as high as 5% (Fig. 5). Therefore, mutants do not need to be single-spore-purified before performing an HRM curve analysis, and multiple mutants can be pooled together for large-scale screens. The observation that mutant DNA can be detected when mixed with wt DNA further reduces the cost and workload of the assay, and further validates the use of an HRM curve analysis for the high throughput screening of CRISPR-Cas9 fungal transformants.

4.4. *CRISPR-Cas9 editing of the* THN *gene does not alter the phenotype of* V. inaequalis *grown in culture*

CRISPR-Cas9-based experiments can sometimes be detrimental to the target organism due to Cas9 toxicity and/or off-target mutations (Morgens et al., 2017), even though CRISPR-Cas9 off-target mutations have been reported to be unlikely in different filamentous fungi (Al Abdallah et al., 2018; Foster et al., 2018; Schuster et al., 2016). To test if CRISPR-Cas9-mediated transformation has greatly affected the phenotype of *V. inaequalis* (e.g. through toxicity or off-target effects), we investigated the phenotypes of the wt, three dark-brown transformants (THN #38, THN #53, THN #90) and six light-brown mutants (THN #9, THN#37, THN#60, THN#66,

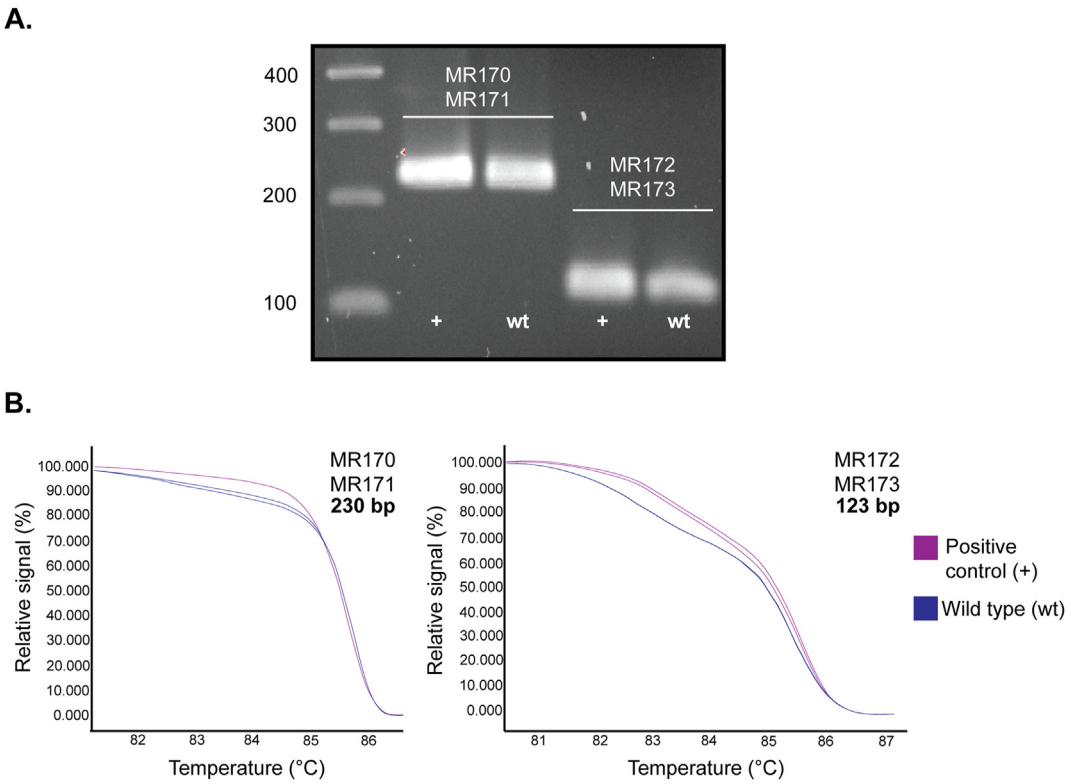

Fig. 3. Optimization of primers for qPCR-HRM curve analysis of the *trihydroxynaphthalene reductase* (*THN*) gene mutants generated using CRISPR-Cas9 sgRNA 4. **A.** Conventional PCR amplification of the *THN* gene positive control (+) and wild type (wt) sequences with the different primer sets resolved by electrophoresis on a 1.5% TBE agarose gel. Ladder sizes are shown in base pairs (bp). **B.** Normalized and shifted melting curves of the *THN* gene positive control (+) and wild type (wt) PCR amplicons generated with two different primer sets (MR170-MR171 and MR172-MR173).

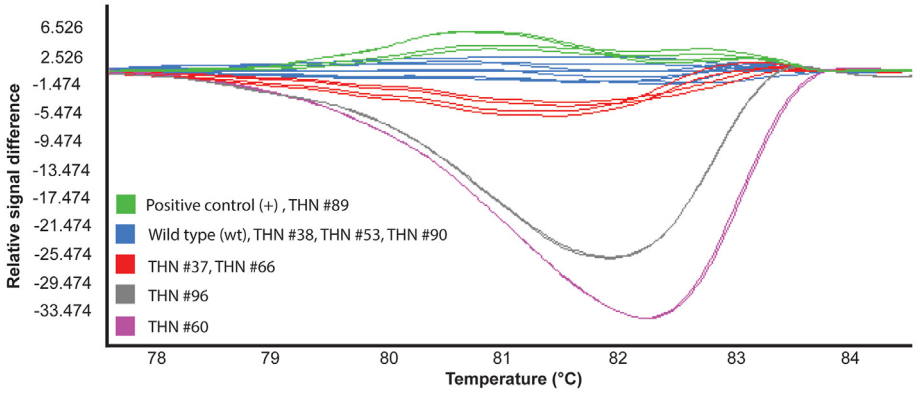

Fig. 4. Screening of CRISPR-Cas9 transformants of *Venturia inaequalis* using qPCR-HRM curve and PCR amplicon sequencing analyses. Plot showing normalized and temperature-shifted differences in melting curves between *trihydroxynaphthalene reductase* (*THN*) amplicons of transformants. Melting curve groups were generated by LightCycler® 480 gene scanning software with a sensitivity of 0.40 and using AccuMelt HRM SuperMix fluorescent dye (DNAture). The experiment is based on two technical replicates per sample.

THN#89, THN#96) of *V. inaequalis* on and in cellophane membranes overlaying PDA. During growth in cellophane membranes, *V. inaequalis* undergoes morphological differentiation, similar to that observed under the cuticle *in planta*, where it develops infection structures called runner hyphae and stromata (Kucheryava et al., 2008). Therefore, we investigated whether the *THN* mutants maintained their ability to develop runner hyphae and stromata in cellophane membranes after CRISPR-Cas9-mediated transformation (Fig. 6). All mutants showed a similar phenotype to wt, in that they were able to penetrate the cellophane membrane to develop runner hyphae and stromata. Likewise, all mutants maintained their ability to sporulate on the cellophane membrane surface. Taken together, these results suggest that CRISPR-Cas9-mediated transformation has not greatly affected the phenotype of *V. inaequalis*. A more in-depth analysis based on whole genome sequencing is the next step to determine whether this experiment has resulted in any off-target mutations.

5. Conclusions

We have successfully applied CRISPR-Cas9 gene editing to the filamentous fungal pathogen, *V. inaequalis*, providing an opportunity for future studies to characterise gene functions associated with the growth, reproduction, virulence and pathogenicity of this

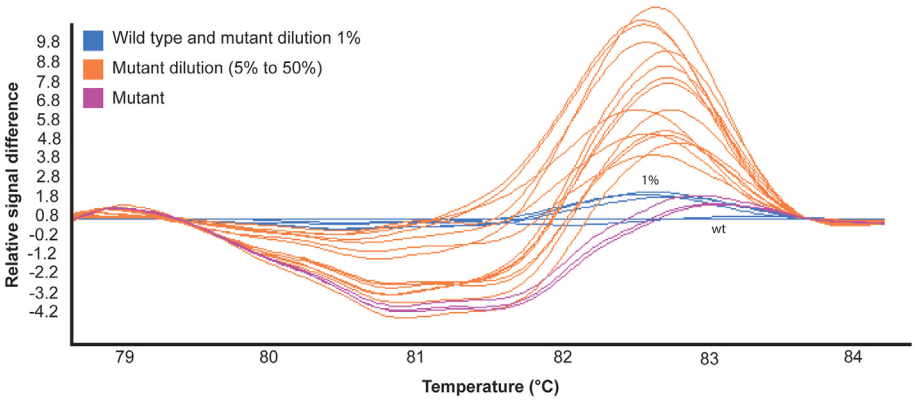

Fig. 5. qPCR-HRM sensitivity to detect a one base pair deletion in mutant−wild type DNA mixtures. Plot showing normalized and temperature-shifted differences in melting curves between wild type (wt) *trihydroxynaphthalene reductase* (*THN*) DNA samples of *V. inaequalis* wt mixed with mutant *THN* DNA samples to detect the resolution limit of the HRM curve assay. Melting curve groups generated by LightCycler® 480 gene scanning software with a sensitivity of 0.48 and using AccuMelt HRM SuperMix fluorescent dye (DNAture). A minimum of two technical replicates were performed per sample. Wt genomic DNA and mutant THN #66 genomic DNA were diluted in different ratios (mutant:wt): 1:99, 5:95, 10:90, 20:80, 30:70 and 50:50.

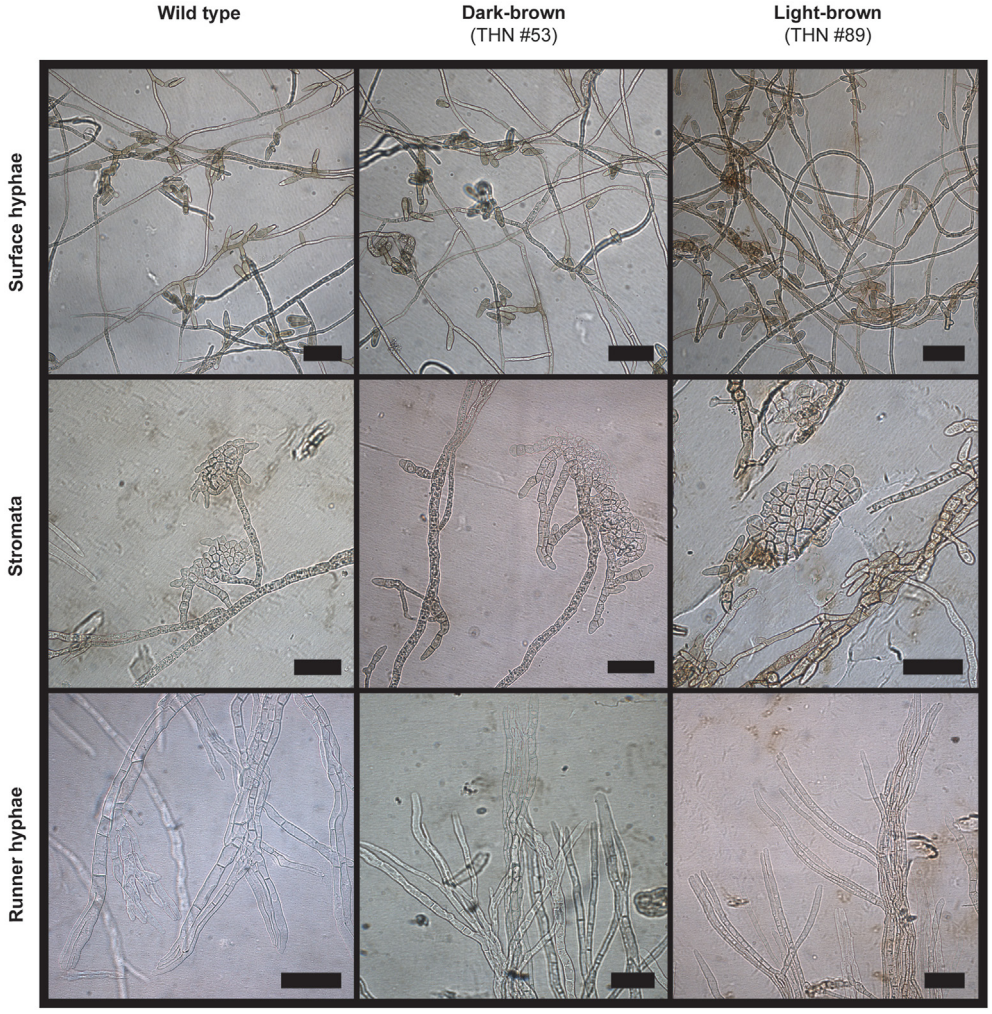

Fig. 6. In-culture phenotype of wild-type and CRISPR-Cas9 transformants of *Venturia inaequalis* on and in a cellophane membrane. The conidia of each strain were plated on a cellophane membrane overlaying potato-dextrose agar, followed by incubation at 22 °C for 10 days. Scale bar 50 μM. Pictures are representative of all *THN* mutants identified.

fungus. Given that the genomes of several other species from the *Venturia* genus have recently been sequenced (Chen et al., 2017; Cooke et al., 2014; Deng et al., 2017; Jaber et al., 2020; Johnson et al., 2019; Prokchorchik et al., 2019; Winter et al., 2020), this development will likely be useful for the functional characterization of genes in these species. Notably, genome sequencing has revealed

that members of the *Venturia* genus contain large, expanded families of putative effector genes that likely play an important role in host colonization (Deng et al., 2017). As the functional characterization of gene families is often hindered by functional redundancy between family members, and because the sequential deletion of family members using standard homologous recombination is limited by the number of selectable marker genes that are available, our finding that CRISPR-Cas9 technology can be applied to *V. inaequalis* is also expected to greatly facilitate the functional characterization of effector gene families in the *Venturia* genus (i.e. through sequential gene deletion/disruption or simultaneous gene targeting (multiplexing)) (Schuster et al., 2018).

In addition to applying CRISPR-Cas9 gene editing to *V. inaequalis*, we have developed a high-throughput screening protocol based on an HRM curve analysis for the identification of CRISPR-Cas9-generated mutants of this fungus with as little as one bp insertion or deletion. We have observed that this highly sensitive method can detect mutant DNA even when mixed in a 5:95 mutant:wt ratio, making it an excellent method for high-throughput screening, as mutants do not need to be single-spore purified prior to screening. This method will be of great value for the identification of mutants generated by CRISPR-Cas9 technology in different fungal species where the mutation efficiency is low.

Funding

MR and CHM are supported by the Marsden Fund Council from Government funding (project ID 17-MAU-100), managed by Royal Society Te Apārangi. SA and JKB received funding from The New Zealand Institute for Plant and Food Research Limited, Strategic Science Investment Fund, Project number: 12070. DH, JS, RDJ and LJJ are supported by the MBIE partnership programme: Novel variation for a persistent problem (project ID C10X1902). AgResearch work was also supported through a QEII technicians' study award (to JS) and the New Zealand Strategic Science Investment Fund (SSIF) contract A20067.

Author contributions

MR, JKB, KMP, REB, RDJ, LJJ and CHM conceptualization; CHM funding acquisition (Marsden Fund); MR, SA, DH and JSS investigation. CHM project administration; JKB, REB and CHM supervision; MR, DH, JKB, KMP, REB, RDJ and CHM roles/writing – original draft; MR, SA, DH, JSS, JKB, KMP, REB, RDJ, LJJ and CHM writing – review & editing.

Declaration of competing interest

The authors declare that they have no known competing financial interests or personal relationships that could have appeared to influence the work reported in this paper.

Acknowledgements

We thank Professor Adrian Tsang (Center for Functional and Structural Genomics Biology, Concordia University, Canada) for hosting JS and providing the original CRISPR-Cas9 vectors. We also thank Natasha Forester and Pranav Chettri for useful discussions around vector modification.

Appendix A. Supplementary data

Supplementary data to this article can be found online at https://doi.org/10.1016/j.funbio.2021.10.001.

References

Al Abdallah, Q., Souza, A.C.O., Martin-Vicente, A., Ge, W., Fortwendel, J.R., 2018. Whole-genome sequencing reveals highly specific gene targeting by in vitro assembled Cas9-ribonucleoprotein complexes in *Aspergillus fumigatus*. Fungal Biol. Biotechnol. 5, 11. https://doi.org/10.1186/s40694-018-0057-2.

Aleksenko, A., Clutterbuck, A.J., 1997. Autonomous plasmid replication in *Aspergillus nidulans*: AMA1 and MATE Elements. Fungal Genet. Biol. 21 (3), 373–387. https://doi.org/10.1006/fgbi.1997.0980.

Bowen, J.K., Mesarich, C.H., Bus, V.G., Beresford, R.M., Plummer, K.M., Templeton, M.D., 2011. *Venturia inaequalis*: the causal agent of apple scab. Mol. Plant Pathol. 12 (2), 105–122. https://doi.org/10.1111/j.1364-3703.2010.00656.x.

Bowen, J.K., Mesarich, C.H., Rees-George, J., Cui, W., Fitzgerald, A., Win, J., Plummer, K.M., Templeton, M.D., 2009. Candidate effector gene identification in the ascomycete fungal phytopathogen *Venturia inaequalis* by expressed sequence tag analysis. Mol. Plant Pathol. 10 (3), 431–448. https://doi.org/10.1111/j.1364-3703.2009.00543.x.

Chen, C., Bock, C.H., Wood, B.W., 2017. Draft genome sequence of *Venturia carpophila*, the causal agent of peach scab. Stand. Genom. Sci. 12, 68. https://doi.org/10.1186/s40793-017-0280-0.

Cooke, I.R., Jones, D., Bowen, J.K., Deng, C., Faou, P., Hall, N.E., Jayachandran, V., Liem, M., Taranto, A.P., Plummer, K.M., Mathivanan, S., 2014. Proteogenomic analysis of the *Venturia pirina* (pear scab fungus) secretome reveals potential effectors. J. Proteome Res. 13 (8), 3635–3644. https://doi.org/10.1021/pr500176c.

Denbow, C.J., Lapins, S., Dietz, N., Scherer, R., Nimchuk, Z.L., Okumoto, S., 2017. Gateway-compatible CRISPR-Cas9 vectors and a rapid detection by high-resolution melting curve analysis. Front. Plant Sci. 8, 1171. https://doi.org/10.3389/fpls.2017.01171.

Deng, C.H., Plummer, K.M., Jones, D.A.B., Mesarich, C.H., Shiller, J., Taranto, A.P., Robinson, A.J., Kastner, P., Hall, N.E., Templeton, M.D., Bowen, J.K., 2017. Comparative analysis of the predicted secretomes of Rosaceae scab pathogens *Venturia inaequalis* and *V. pirina* reveals expanded effector families and putative determinants of host range. BMC Genom. 18 (1), 339. https://doi.org/10.1186/s12864-017-3699-1.

DiCarlo, J.E., Norville, J.E., Mali, P., Rios, X., Aach, J., Church, G.M., 2013. Genome engineering in *Saccharomyces cerevisiae* using CRISPR-Cas systems. Nucleic Acids Res. 41 (7), 4336–4343. https://doi.org/10.1093/nar/gkt135.

Doench, J.G., Hartenian, E., Graham, D.B., Tothova, Z., Hegde, M., Smith, I., Sullender, M., Ebert, B.L., Xavier, R.J., Root, D.E., 2014. Rational design of highly active sgRNAs for CRISPR-Cas9–mediated gene inactivation. Nat. Biotechnol. 32 (12), 1262–1267. https://doi.org/10.1038/nbt.3026.

Doudna, J.A., Charpentier, E., 2014. The new frontier of genome engineering with CRISPR-Cas9. Science 346 (6213), 1258096. https://doi.org/10.1126/science.1258096.

Dufresne, S.D., Belloni, D.R., Wells, W.A., Tsongalis, G.J., 2006. *BRCA1* and *BRCA2* mutation screening using SmartCycler II high-resolution melt curve analysis. *Arch. Pathol. Lab Med*. 130 (2), 185–187. https://doi.org/10.1043/1543-2165(2006)130[185:BABMSU]2.0.CO;2.

Fang, Y., Tyler, B.M., 2016. Efficient disruption and replacement of an effector gene in the oomycete *Phytophthora sojae* using CRISPR/Cas9. Mol. Plant Pathol. 17 (1), 127–139. https://doi.org/10.1111/mpp.12318.

Feurtey, A., Guitton, E., De Gracia Coquerel, M., Duvaux, L., Shiller, J., Bellanger, M.-N., Expert, P., Sannier, M., Caffier, V., Giraud, T., Le Cam, B., Lemaire, C., 2020. Threat to Asian wild apple trees posed by gene flow from domesticated apple trees and their "pestified" pathogens. Mol. Ecol. 29 (24), 4925–4941. https://doi.org/10.1111/mec.15677.

Fitzgerald, A., van Kan, J.A., Plummer, K.M., 2004. Simultaneous silencing of multiple genes in the apple scab fungus, *Venturia inaequalis*, by expression of RNA with chimeric inverted repeats. Fungal Genet. Biol. 41 (10), 963–971. https://doi.org/10.1016/j.fgb.2004.06.006.

Fitzgerald, A.M., Mudge, A.M., Gleave, A.P., Plummer, K.M., 2003. *Agrobacterium* and PEG-mediated transformation of the phytopathogen *Venturia inaequalis*. Mycol. Res. 107 (7), 803–810. https://doi.org/10.1017/S0953756203008086.

Fleetwood, D.J., Scott, B., Lane, G.A., Tanaka, A., Johnson, R.D., 2007. A complex ergovaline gene cluster in *Epichloë* endophytes of grasses. Appl. Environ. Microbiol. 73 (8), 2571. https://doi.org/10.1128/AEM.00257-07.

Foster, A.J., Martin-Urdiroz, M., Yan, X., Wright, H.S., Soanes, D.M., Talbot, N.J., 2018. CRISPR-Cas9 ribonucleoprotein-mediated co-editing and counterselection in the rice blast fungus. Sci. Rep. 8 (1), 14355. https://doi.org/10.1038/s41598-018-32702-w.

González-Domínguez, E., Armengol, J., Rossi, V., 2017. Biology and epidemiology of *Venturia* species affecting fruit crops: a review. Front. Plant Sci. 8, 1496. https://doi.org/10.3389/fpls.2017.01496.

Hamada, W., Reignault, P., Bompeix, G., Boccara, M., 1994. Transformation of *Botrytis cinerea* with the hygromycin B resistance gene, *hph*. Curr. Genet. 26 (3), 251–255. https://doi.org/10.1007/BF00309556.

Idnurm, A., Urquhart, A.S., Vummadi, D.R., Chang, S., van de Wouw, A.P., López-Ruiz, F.J., 2017. Spontaneous and CRISPR/Cas9-induced mutation of the osmosensor histidine kinase of the canola pathogen *Leptosphaeria maculans*. Fungal Biol. Biotechnol. 4, 12. https://doi.org/10.1186/s40694-017-0043-0.

Jaber, M.Y., Bao, J., Gao, X., Zhang, L., He, D., Wang, X., Wang, A., Wang, Z., Wang, B., 2020. Genome sequence of *Venturia oleaginea*, the causal agent of olive leaf scab. Mol. Plant Microbe Interact. 33 (9), 1095–1097. https://doi.org/10.1094/MPMI-03-20-0070-A.

Jha, G., Thakur, K., Thakur, P., 2009. The *Venturia* apple pathosystem: pathogenicity mechanisms and plant defense responses. J. Biomed. Biotechnol. https://doi.org/10.1155/2009/680160, 2009, 680160.

Johnson, S., Jones, D., Thrimawithana, A.H., Deng, C.H., Bowen, J.K., Mesarich, C.H., Ishii, H., Won, K., Bus, V.G.M., Plummer, K.M., 2019. Whole genome sequence resource of the Asian pear scab pathogen *Venturia nashicola*. Mol. Plant Microbe Interact. 32 (11), 1463–1467. https://doi.org/10.1094/MPMI-03-19-0067-A.

Kearse, M., Moir, R., Wilson, A., Stones-Havas, S., Cheung, M., Sturrock, S., Buxton, S., Cooper, A., Markowitz, S., Duran, C., Thierer, T., Ashton, B., Meintjes, P., Drummond, A., 2012. Geneious Basic: an integrated and extendable desktop software platform for the organization and analysis of sequence data. Bioinformatics 28 (12), 1647–1649. https://doi.org/10.1093/bioinformatics/bts199.

Khan, H., McDonald, M.C., Williams, S.J., Solomon, P.S., 2020. Assessing the efficacy of CRISPR/Cas9 genome editing in the wheat pathogen *Parastagonspora nodorum*. Fungal Biol. Biotechnol. 7 (1), 4. https://doi.org/10.1186/s40694-020-00094-0.

Krappmann, S., 2007. Gene targeting in filamentous fungi: the benefits of impaired repair. Fungal Biol. Rev. 21 (1), 25–29. https://doi.org/10.1016/j.fbr.2007.02.004.

Krappmann, S., 2017. CRISPR-Cas9, the new kid on the block of fungal molecular biology. Med. Mycol. 55 (1), 16–23. https://doi.org/10.1093/mmy/myw097.

Kucheryava, N., Bowen, J.K., Sutherland, P.W., Conolly, J.J., Mesarich, C.H., Rikkerink, E.H., Kemen, E., Plummer, K.M., Hahn, M., Templeton, M.D., 2008. Two novel *Venturia inaequalis* genes induced upon morphogenetic differentiation during infection and *in vitro* growth on cellophane. Fungal Genet. Biol. 45 (10), 1329–1339. https://doi.org/10.1016/j.fgb.2008.07.010.

Le Cam, B., Sargent, D., Gouzy, J., Amselem, J., Bellanger, M.-N., Bouchez, O., Brown, S., Caffier, V., De Gracia, M., Debuchy, R., Duvaux, L., Payen, T., Sannier, M., Shiller, J., Collemare, J., Lemaire, C., 2019. Population genome gequencing of the scab fungal species *Venturia inaequalis, Venturia pirina, Venturia aucupariae* and *Venturia asperata*. G3-Genes Genom. Genet. 9 (8), 2405–2414. https://doi.org/10.1534/g3.119.400047.

Li, R., Ba, Y., Song, Y., Cui, J., Zhang, X., Zhang, D., Yuan, Z., Yang, L., 2020. Rapid and sensitive screening and identification of CRISPR/Cas9 edited rice plants using quantitative real-time PCR coupled with high resolution melting analysis. Food Control 112, 107088. https://doi.org/10.1016/j.foodcont.2020.107088.

Lichtner, F.J., Jurick, W.M., Ayer, K.M., Gaskins, V.L., Villani, S.M., Cox, K.D., 2020. A genome resource for several North American *Venturia inaequalis* isolates with multiple fungicide resistance phenotypes. Phytopathology 110 (3), 544–546. https://doi.org/10.1094/PHYTO-06-19-0222-A.

Mesarich, C.H., Schmitz, M., Tremouilhac, P., McGillivray, D.J., Templeton, M.D., Dingley, A.J., 2012. Structure, dynamics and domain organization of the repeat protein Cin1 from the apple scab fungus. Biochim. Biophys. Acta Protein Proteonomics 1824 (10), 1118–1128. https://doi.org/10.1016/j.bbapap.2012.06.015.

Morgens, D.W., Wainberg, M., Boyle, E.A., Ursu, O., Araya, C.L., Tsui, C.K., Haney, M.S., Hess, G.T., Han, K., Jeng, E.E., Li, A., Snyder, M.P., Greenleaf, W.J., Kundaje, A., Bassik, M.C., 2017. Genome-scale measurement of off-target activity using Cas9 toxicity in high-throughput screens. Nat. Commun. 8 (1), 15178. https://doi.org/10.1038/ncomms15178.

Nakayashiki, H., Nguyen, Q.B., 2008. RNA interference: roles in fungal biology. Curr. Opin. Microbiol. 11 (6), 494–502. https://doi.org/10.1016/j.mib.2008.10.001.

Nødvig, C.S., Hoof, J.B., Kogle, M.E., Jarczynska, Z.D., Lehmbeck, J., Klitgaard, D.K., Mortensen, U.H., 2018. Efficient oligo nucleotide mediated CRISPR-Cas9 gene editing in Aspergilli. Fungal Genet. Biol. 115, 78–89. https://doi.org/10.1016/j.fgb.2018.01.004.

Nødvig, C.S., Nielsen, J.B., Kogle, M.E., Mortensen, U.H., 2015. A CRISPR-Cas9 system for genetic engineering of filamentous fungi. PLoS One 10 (7), e0133085. https://doi.org/10.1371/journal.pone.0133085.

Papp, D., Singh, J., Gadoury, D., Khan, A., 2020. New North American isolates of *Venturia inaequalis* can overcome apple scab resistance of *Malus floribunda* 821. Plant Dis. 104 (3), 649–655. https://doi.org/10.1094/PDIS-10-19-2082-RE.

Passey, T.A.J., Armitage, A.D., Sobczyk, M.K., Shaw, M.W., Xu, X., 2020. Genomic sequencing indicates non-random mating of *Venturia inaequalis* in a mixed cultivar orchard. Plant Pathol. 69 (4), 669–676. https://doi.org/10.1111/ppa.13150.

Passey, T.A.J., Armitage, A.D., Xu, X., 2018. Annotated draft genome sequence of the apple scab pathogen *Venturia inaequalis*. Microbiol. Resour. Announc. 7 (12). https://doi.org/10.1128/MRA.01062-18 e01062-18.

Prokchorchik, M., Won, K., Lee, Y., Choi, E.D., Segonzac, C., Sohn, K.H., 2019. High contiguity whole genome sequence and gene annotation resource for two *Venturia nashicola* isolates. Mol. Plant Microbe Interact. 32 (9), 1091–1094. https://doi.org/10.1094/MPMI-03-19-0072-A.

Rahnama, M., Forester, N., Ariyawansa, K.G.S.U., Voisey, C.R., Johnson, L.J., Johnson, R.D., Fleetwood, D.J., 2017. Efficient targeted mutagenesis in *Epichloë festucae* using a split marker system. J. Microbiol. Methods 134, 62–65. https://doi.org/10.1016/j.mimet.2016.12.017.

Reed, G.H., Wittwer, C.T., 2004. Sensitivity and specificity of single-nucleotide polymorphism scanning by high-resolution melting analysis. Clin. Chem. 50 (10), 1748–1754. https://doi.org/10.1373/clinchem.2003.029751.

Salame, T.M., Ziv, C., Hadar, Y., Yarden, O., 2011. RNAi as a potential tool for biotechnological applications in fungi. Appl. Microbiol. Biotechnol. 89 (3), 501–512. https://doi.org/10.1007/s00253-010-2928-1.

Sánchez-Torres, P., González, R., Pérez-González, J.A., González-Candelas, L., Ramón, D., 1994. Development of a transformation system for *Trichoderma longibrachiatum* and its use for constructing multicopy transformants for the *egl1* gene. Appl. Microbiol. Biotechnol. 41 (4), 440–446. https://doi.org/10.1007/BF01982533.

Sander, J.D., Joung, J.K., 2014. CRISPR-Cas systems for editing, regulating and targeting genomes. Nat. Biotechnol. 32 (4), 347–355. https://doi.org/10.1038/nbt.2842.

Schuster, M., Kahmann, R., 2019. CRISPR-Cas9 genome editing approaches in filamentous fungi and oomycetes. Fungal Genet. Biol. 130, 43–53. https://doi.org/10.1016/j.fgb.2019.04.016.

Schuster, M., Schweizer, G., Kahmann, R., 2018. Comparative analyses of secreted proteins in plant pathogenic smut fungi and related basidiomycetes. Fungal Genet. Biol. 112, 21–30. https://doi.org/10.1016/j.fgb.2016.12.003.

Schuster, M., Schweizer, G., Reissmann, S., Kahmann, R., 2016. Genome editing in *Ustilago maydis* using the CRISPR–Cas system. Fungal Genet. Biol. 89, 3–9. https://doi.org/10.1016/j.fgb.2015.09.001.

Shi, T.Q., Liu, G.N., Ji, R.Y., Shi, K., Song, P., Ren, L.J., Huang, H., Ji, X.-J., 2017. CRISPR/Cas9-based genome editing of the filamentous fungi: the state of the art. Appl. Microbiol. Biotechnol. 101 (20), 7435–7443. https://doi.org/10.1007/s00253-017-8497-9.

Shiller, J., van de Wouw, A.P., Taranto, A.P., Bowen, J.K., Dubois, D., Robinson, A., Deng, C.H., Plummer, K.M., 2015. A large family of *AvrLm6-like* genes in the apple and pear scab pathogens, *Venturia inaequalis* and *Venturia pirina*. Front. Plant Sci. 6, 980. https://doi.org/10.3389/fpls.2015.00980.

Simko, I., 2016. High-resolution DNA melting analysis in plant research. Trends Plant Sci. 21 (6), 528–537. https://doi.org/10.1016/j.tplants.2016.01.004.

Słomka, M., Sobalska-Kwapis, M., Wachulec, M., Bartosz, G., Strapagiel, D., 2017. High Resolution Melting (HRM) for high-throughput genotyping—limitations and caveats in practical case studies. Int. J. Mol. Sci. 18 (11), 2316. https://doi.org/10.3390/ijms18112316.

Song, L., Ouedraogo, J.-P., Kolbusz, M., Nguyen, T.T.M., Tsang, A., 2018. Efficient genome editing using tRNA promoter-driven CRISPR/Cas9 gRNA in *Aspergillus niger*. PLoS One 13 (8). https://doi.org/10.1371/journal.pone.0202868 e0202868-e.

Stehmann, C., Pennycook, S., Plummer, K.M., 2001. Molecular identification of a sexual interloper: the pear pathogen, *Venturia pirina*, has sex on apple. Phytopathology 91 (7), 633–641. https://doi.org/10.1094/PHYTO.2001.91.7.633.

Vouillot, L., Thélie, A., Pollet, N., 2015. Comparison of T7E1 and surveyor mismatch cleavage assays to detect mutations triggered by engineered nucleases. G3-Genes Genom. Genet. 5 (3), 407–415. https://doi.org/10.1534/g3.114.015834.

Winter, D.J., Charlton, N.D., Krom, N., Shiller, J., Bock, C.H., Cox, M.P., Young, C.A., 2020. Chromosome-level reference genome of *Venturia effusa*, causative agent of pecan scab. Mol. Plant Microbe Interact. 33 (2), 149–152. https://doi.org/10.1094/MPMI-08-19-0236-A.

Wittwer, C.T., 2009. High-resolution DNA melting analysis: advancements and limitations. Hum. Mutat. 30 (6), 857–859. https://doi.org/10.1002/humu.20951.

Zhu, X., Xu, Y., Yu, S., Lu, L., Ding, M., Cheng, J., Song, G., Gao, X., Yao, L., Fan, D., Meng, S., Zhang, X., Hu, S., Tian, Y., 2014. An efficient genotyping method for genome-modified animals and human cells generated with CRISPR/Cas9 system. Sci. Rep. 4 (1), 6420. https://doi.org/10.1038/srep06420.